XI International Conference on Computational Plasticity. Fundamentals and Applications
COMPLAS XI
E. Oñate, D.R.J. Owen, D. Peric and B. Suárez (Eds)

COMPUTATIONAL HOMOGENIZATION FOR TWO-SCALE MODELING OF PERFUSED TISSUES

EDUARD ROHAN AND VLADIMÍR LUKEŠ

Department of Mechanics, Faculty of Applied Sciences, University of West Bohemia,
Univerzitní 22, 306 14 Plzeň, Czech Republic, e-mail: rohan@kme.zcu.cz

Key words: Perfusion, Homogenization, Porous Media, Large Deformation

Abstract. We developed a two-scale approach for modeling large-deforming perfused media with the 3-compartment microstructure. An incremental formulation based on the updated Lagrangian configuration and the Biot-type continuum model is introduced. Equations of the model express mechanical equilibrium and the volume fluid redistribution (the Darcy law), assuming both the fluid and solid phases are incompressible. This linearized system was treated by the homogenization method assuming locally periodic structures. The local reference cell involving geometrical representations of the blood vessels evolves in time due to large deformation. The homogenized model is implemented using a finite element code and a numerical example is presented.

1 INTRODUCTION

Modeling of tissue perfusion is one of the most challenging issues in biomechanics. There are several hurdles originating in structural arrangement of the so-called perfusion tree, necessity of bridging several scales, the blood flow descriptions depending on the scale, and fluid-structure interactions. We focus on modeling the perfusion of deforming tissue parenchym. At the level of small vessels and microvessels, the perfusion can be described using the Darcy flow in a double-porous structure consisting of 3 compartments: two disconnected channels (small arteries and veins) and the matrix (microvessels and capillaries), represented as the dual porosity, where the permeability is decreasing with the scale parameter the size of the microstructure. In some kinds of tissues, the coupling between flow (fluid diffusion) and deformation is quite important, cf. [7] where the case of linear deformation is described. In this short communication we present a perfusion model of the homogenized large deforming medium whereby the incremental formulation based on the updated Lagrangian formulation is employed.

The computational algorithm can be characterized as the cycle comprising the following steps: 1) for given reference microstructure - the local configuration (LC) - compute the local response functions and the effective constitutive parameters, 2) compute the

macroscopic response (MR) for given external loads, 3) compute the deformation and stresses at each reference microstructure using MR and update the LC. This algorithm is now implemented in the Sfepy code [1] and tested on 2D examples.

2 LARGE DEFORMING MEDIA AND HOMOGENIZATION

Problems involving nonlinear partial differential equations are difficult to solve in general, therefore, their homogenization by asymptotic analysis with respect to the scale of heterogeneities is quite cumbersome, in general. We follow an approach which is based on homogenization of linear subproblems arising from an incremental formulation associated with the numerical treatment, see [8] and [3, 4, 5]. The homogenization procedure can be described by the following steps:

- A reference configuration at time t is considered. The configuration is defined by locally periodic structure and by the reference state in the form of bounded two-scale functions.
- The homogenization is applied to the linear subproblem: given the configuration at time t, compute the increments associated with time increment Δt, see Section 2.2. The locally periodic microstructure (see Section 2.1) and the reference state define the oscillating coefficients of the linearized equations. Then the standard homogenization [2] can be applied, such that on solving local microscopic problems, the characteristic responses are obtained and the homogenized coefficients can be evaluated at any "macroscopic position" x, as reported in Sections 3.1 and 3.2.
- The homogenized subproblem can be solved at the macroscopic level, thus the increments of the macroscopic response are obtained, see Section 3.3.
- In order to establish new microscopic configurations at time $t + \Delta t$ and at "any" macroscopic position, the macroscopic response is combined with the local microscopic characteristic responses to update the local microscopic states, see Section 3.4. Then the next time step can be considered and the whole procedure repeats.

In contrast with linear problems, where the microscopic responses are solved only once (even though they can depend on time [6, 7]), in nonlinear problems the local microscopic problems must be solved for any iteration (time step) and at "any" macroscopic point, [3, 4, 5]. In fact, the homogenization leads to a two-scale domain decomposition: the macroscopic domain is decomposed into locally representative cells where the microscopic problems must be solved. The data (i.e. the solutions) are passed between the two levels after any iteration (the time increment step), so that the problem remains fairly two-scale during the whole solution procedure. This is the major difficulty which affects directly the complexity of the numerical treatment.

2.1 Locally periodic microstructures and scale separation

Homogenization methods based on the asymptotic analysis of a system of partial differential equation employ the concept of locally almost periodic microstructures. Let ε be the scale which is the ratio between the "microscopic" and the "macroscopic" characteristic lengths. Later we shall need material parameters defined in the local microscopic cell Y^ε using the coordinate split

$$x = \xi^\varepsilon + \varepsilon y \ , \quad y \in Y^\varepsilon(x) \ ,$$

where ξ^ε is the lattice coordinate. The unfolding operation denoted by $\tilde{}$, which enables to rewrite any function of x as a function of two variables: $\phi^\varepsilon(x) = \tilde{\phi}^\varepsilon(\xi^\varepsilon, y)$. The assumption of the local periodicity means that for $\varepsilon \to 0$ the following holds:

(i) $Y^\varepsilon(x) \to Y(x)$,

(ii) $\phi^\varepsilon(x) \to \tilde{\phi}(x, y)$ for a.a. $x \in \Omega$ and $y \in Y(x)$,

where $Y(x)$ is the local reference cell. The scale separation is achieved in the limit $\varepsilon \to 0$. It means that the macroscopic position $x \in \Omega$ is associated with a local periodic microstructure — a periodic array of cells, which are defined by translations of $Y(x)$.

Obviously, a real problem is characterized by a given finite scale ε_0, so that the "absolute" scale separation does not hold. However, the limit problem obtained as $\varepsilon \to 0$ and its solution computed by solving the homogenized equations (see below) can be employed to construct an approximation of the original problem featured by ε_0. For this some postprocessing based on averaging operators can be used.

We shall introduce the following decomposition of Y into the sectors of primary and dual porosities, *cf.* [7]. Let Y_α, $\alpha = 1, 2$ be two disjoint subdomains of Y with Lipschitz boundary, such that $\partial_\alpha Y_\alpha := \overline{Y_\alpha} \cap \partial Y \neq \emptyset$ is formed by mutually homologous points of ∂Y, see Fig. 1 (right); this is necessary to have connected channels. The periodic array obtained by translating Y_α forms a connected domains.

Further by $Y_3 = Y \setminus (\overline{Y_1} \cup \overline{Y_2})$ we denote the "matrix", which thus separates the channels Y_1 and Y_2. Domain Y_3 is associated with the dual porosity, where the permeability is very small, see equation (4). By $\Gamma_\beta = \partial Y_\beta \cap \partial Y_3$ we denote the channel-matrix interface.

2.2 Updated Lagrangian formulation

In order to define the weak formulation for the linearized deformation-diffusion problem, we need some preliminaries. Let $\partial_D\Omega \subset \partial\Omega$ be the part of the boundary where the zero displacements are prescribed. Now we define $\boldsymbol{V}_0(\Omega) = \{\boldsymbol{v} \in W^{1,2}(\Omega)^3 \mid v_i = 0 \text{ on } \partial_D\Omega, i = 1, \ldots, 3\}$ for 3D problems.

In what follows we denote by superscript ε all the quantities which vary with heterogeneities. The micromodel incorporates the following material parameters. The elasticity tensor $D^{\text{eff}\,\varepsilon}_{ijkl}$ is the Truesdell rate of the effective Kirchhoff stress $\tau^{\text{eff},\varepsilon}_{ij}$, which is associated

with a given strain energy function. Denoting by F^ε_{ij} the deformation gradient, $J^\varepsilon = \det F^\varepsilon_{ij}$. Both $D^{\mathrm{eff}\,\varepsilon}_{ijkl}$ and $\tau^{\mathrm{eff}\,\varepsilon}_{ij}$ are functions of F^ε_{ij}, namely $\tau^{\mathrm{eff},\varepsilon}_{ij} = \mu^\varepsilon (J^\varepsilon)^{-2/3}\,\mathrm{dev}(F^\varepsilon_{ik}F^\varepsilon_{jk})$. The Green-Lagrange strain w.r.t. the updated configuration consists of the linear part $\boldsymbol{e} = (e_{ij})$ and the nonlinear part $\boldsymbol{\eta} = (\eta_{ij})$. The porous properties of the medium are described by the symmetric positive definite permeability tensor K^ε_{ij}.

The incremental "algorithmic" approach of time stepping is adhered to formulate the evolution problem for the porous medium. We consider the subproblem of computing the new configuration at time $t + \Delta t$, given a finite time step Δt and the configuration $\mathcal{C}^{\varepsilon,(t)}$ at time t, which is determined by the triplet $\{\Omega, F^\varepsilon_{ij}(x), p^\varepsilon(x)\}(t)$ for $x \in \Omega$.

Let $L^{\mathrm{new}}(\boldsymbol{v})$ be the functional involving the instantaneous boundary and volume forces at time $t + \Delta t$. The finite increments of displacement $\Delta\boldsymbol{u}^\varepsilon \in \boldsymbol{V}_0(\Omega)$ and hydrostatic pressure $\Delta p^\varepsilon \in L^2(\Omega)$ verify the variational equations (1)-(2) which express respectively the balance of stresses – quasi-static equilibrium equation (notation: $\boldsymbol{I} = \delta_{ij}$, $\mathbb{I} = 1/2(\delta_{ik}\delta_{jl} + \delta_{il}\delta_{jk})$, $\boldsymbol{\eta}(\boldsymbol{v}) = (\partial v_k/\partial x_i)(\partial v_k/\partial x_j)$, $\mathbb{D} = (D_{ijkl})$ and $\boldsymbol{\tau} = (\tau_{ij})$)

$$\begin{aligned}
&\int_\Omega [\mathbb{D}^{\mathrm{eff},\varepsilon} : \boldsymbol{e}(\Delta\boldsymbol{u}^\varepsilon)] : \boldsymbol{e}(\boldsymbol{v}^\varepsilon)(J^\varepsilon)^{-1}\mathrm{d}x + \int_\Omega \boldsymbol{\tau}^{\mathrm{eff},\varepsilon} : \delta\boldsymbol{\eta}(\Delta\boldsymbol{u}^\varepsilon;\boldsymbol{v}^\varepsilon)(J^\varepsilon)^{-1}\mathrm{d}x \\
&- \int_\Omega \Delta p^\varepsilon\,\mathrm{div}\boldsymbol{v}^\varepsilon\mathrm{d}x + \int_\Omega p^\varepsilon \nabla(\Delta\boldsymbol{u}^\varepsilon) : (\mathbb{I} - \boldsymbol{I}\otimes\boldsymbol{I}) : \nabla\boldsymbol{v}^\varepsilon\mathrm{d}x \qquad (1)\\
=&L(\boldsymbol{v}^\varepsilon) - \int_\Omega \boldsymbol{\tau}^\varepsilon : \boldsymbol{e}(\boldsymbol{v}^\varepsilon)(J^\varepsilon)^{-1}\mathrm{d}x \qquad\qquad \forall\boldsymbol{v}^\varepsilon \in V(\Omega)\ ,
\end{aligned}$$

where the total Kirchhoff stress is $\tau^\varepsilon_{ij} = -J^\varepsilon\delta_{ij}\ p^\varepsilon + \tau^{\mathrm{eff},\varepsilon}_{ij}$, and the Darcy flow in the dual-porous structure

$$\int_\Omega q^\varepsilon\,\mathrm{div}\Delta\boldsymbol{u}^\varepsilon\mathrm{d}x + \Delta t\int_\Omega \boldsymbol{K}^\varepsilon\cdot\nabla(p^\varepsilon + \Delta p^\varepsilon)\cdot\nabla q^\varepsilon\mathrm{d}x = 0\ , \quad \forall q^\varepsilon \in H^1(\Omega)\ . \qquad (2)$$

3 PERFUSION IN LARGE DEFORMING POROUS MEDIA

The material parameters in deformed configuration depend on the deformation gradient $F^\varepsilon_{ij}(x)$. Within the *updated Lagrangian formulation* we use the coordinates in the deformed reference configuration. At the microscopic scale, we establish the *local deformed configuration*: For $x \in \Omega$, let $\tilde{F}_{ij}(x,y)$, $y \in Y(x)$ be the two-scale limit of the deformation gradient associated with the mapping of the corresponding initial (undeformed) reference cell onto $Y(x)$. Then the local microscopic configuration at time t is the triplet

$$\mathcal{C}^{(t)}(x) = \{Y^{(t)}(x), \tilde{F}^{(t)}_{ij}(x,y), \tilde{p}^{(t)}(x,y) | y \in Y^{(t)}(x)\}\ . \qquad (3)$$

We assume that at any such configuration we may establish locally periodic material parameters. The permeability is defined using the dual porosity ansatz (for homogenization) characterized by ε^2 scaling of the permeability coefficients in the "matrix":

$$K^\varepsilon_{ij}(x) := \begin{cases} \tilde{K}^\alpha_{ij}(x,y) & y \in Y_\alpha,\ \alpha = 1,2\ , \\ \varepsilon^2\tilde{K}^3_{ij}(x,y) & y \in Y_3\ . \end{cases} \qquad (4)$$

Obviously, tensors $\tilde{K}_{ij}$ depend on the material deformation and should be modified from one time level to the next one using $\tilde{F}$, as will be discussed in Section 3.4.

Further we define tangent modulus $\tilde{\mathbb{A}} = (\tilde{A}_{ijkl})$ which depends on $\tilde{F}_{ij}$ (through $\tilde{D}^{\rm eff}_{ijkl}$ and $\tilde{\tau}^{\rm eff}_{jl}$) and on the interstitial fluid pressure $\tilde{p}$,

$$\tilde{A}_{ijkl}(x,y) = \left(\tilde{D}^{\rm eff}_{ijkl} + \tilde{\tau}^{\rm eff}_{jl}\delta_{ki} + \tilde{J}\tilde{p}\,(\delta_{jk}\delta_{il} - \delta_{ij}\delta_{kl})\right)\ , \tag{5}$$

where all quantities denoted by $\tilde{}$ are expressed for $x \in \Omega$ as locally periodic functions of $y \in Y(x)$.

3.1 Asymptotic expansions and corrector basis functions

The linearized problem can be treated using standard homogenization methods, such as the periodic unfolding, the two-scale convergence, or even the asymptotic expansion methods. The fluctuating fields $\Delta\boldsymbol{u}^\varepsilon$ and Δp^ε can be expressed by the following asymptotic expansions:

$$\begin{aligned}
\Delta\boldsymbol{u}^\varepsilon(x) &= \Delta\boldsymbol{u}^0(x) + \varepsilon\Delta\boldsymbol{u}^1(x,y) + O(\varepsilon^2)\ ,\\
\Delta p^\varepsilon(x) &= \sum_{\alpha=1,2}\chi_\alpha(y)\left(\Delta p^0_\alpha(x) + \varepsilon\Delta p^1_\alpha(x,y) + O(\varepsilon^2)\right) + \chi_3(y)\left(\Delta\tilde{p}_3(x,y) + O(\varepsilon)\right)\ ,
\end{aligned} \tag{6}$$

where $y \in Y(x)$, $\chi_s(y)$, $s = 1,2,3$ are characteristic functions of subdomains Y_s and all functions are Y-periodic in variable y. For this we established appropriate spaces:

$$\begin{aligned}
H^1_{\#}(Y_\alpha) &= \{v \in H^1(Y_\alpha)\ ,\ v \text{ is Y-periodic, } \int_{Y_\alpha} v = 0\}\ ,\\
H^1_{\#0}(Y_3) &= \{v \in H^1(Y_3)\ ,\ v \text{ is Y-periodic, } v = 0 \text{ on } \Gamma_\alpha\}\ .
\end{aligned} \tag{7}$$

The fluctuating parts of the displacements and pressures are expressed in terms of the corrector basis functions: we introduce Y-periodic functions $\boldsymbol{\omega}^{rs}, \boldsymbol{\omega}^\alpha, \boldsymbol{u}^P \in \mathbf{H}^1_{\#}(Y)$, $\pi^{rs}, p^P \in H^1_{\#0}(Y_3)$, $\pi^\alpha \in H^1_{\#}(Y_3)$, $\eta^k_\alpha \in H^1_{\#}(Y_\alpha)$,

$$\begin{aligned}
\Delta\boldsymbol{u}^1 &= \boldsymbol{\omega}^{rs}\partial^x_s\Delta u_r + \sum_{\alpha=1,2}\boldsymbol{\omega}^\alpha\Delta p^0_\alpha + \boldsymbol{u}^P\ ,\\
\Delta\tilde{p}_3 &= \pi^{rs}\partial^x_s\Delta u_r + \sum_{\alpha=1,2}\pi^\alpha\Delta p^0_\alpha + p^P\ ,\\
\Delta p^1_\alpha &= \eta^k_\alpha\partial^x_k\Delta p^0_\alpha\ ,\quad \alpha = 1,2\ ,
\end{aligned} \tag{8}$$

due to the "channel-matrix interface" conditions, $\pi^\alpha = \delta_{\alpha\beta}$ on Γ_β.

3.2 Local microscopic problems

We shall need the following notation to introduce the local microscopic problems:

$$a_Y(\boldsymbol{u},\,\boldsymbol{v}) = \int_Y \tilde{A}_{ijkl}\partial^y_l u_k\partial^y_j v_i\tilde{J}^{-1}{\rm d}y\ ,\qquad c_{Y_k}(p,\,q) = \int_{Y_k}(\tilde{\boldsymbol{K}}^k\cdot\nabla_y p)\cdot\nabla_y q\,{\rm d}y\ , \tag{9}$$

where $k = 1, 2, 3$. These bilinear forms depend on $\mathcal{C}^{(t)}(x)$ for $x \in \Omega$, see (3). The following microscopic problems must be solved:

1. Correctors w.r.t $\partial_s^x \Delta u_r$: find $(\boldsymbol{\omega}^{rs}, \pi^{rs}) \in \mathbf{H}^1_\#(Y) \times H^1_{\#0}(Y_3)$ satisfying

$$\begin{aligned} a_Y\left(\boldsymbol{\omega}^{rs} + \boldsymbol{\Pi}^{rs},\, \boldsymbol{v}\right) - \langle \pi^{rs},\, \mathrm{div}_y \boldsymbol{v}\rangle_{Y_3} = 0\,, \quad \forall \boldsymbol{v} \in \mathbf{H}^1_\#(Y) \\ \langle q,\, \mathrm{div}_y[\boldsymbol{\omega}^{rs} + \boldsymbol{\Pi}^{rs}]\rangle_{Y_3} + \Delta t\, c_{Y_3}\left(\pi^{rs},\, q\right) = 0\,, \quad \forall q \in H^1_{\#0}(Y_3)\,. \end{aligned} \tag{10}$$

2. Correctors w.r.t Δp_α: find $(\boldsymbol{\omega}^\alpha, \pi^\alpha) \in \mathbf{H}^1_\#(Y) \times H^1_\#(Y_3)$ satisfying

$$\begin{aligned} a_Y\left(\boldsymbol{\omega}^\alpha,\, \boldsymbol{v}\right) - \langle \pi^\alpha,\, \mathrm{div}_y \boldsymbol{v}\rangle_{Y_3} = \int_{\Gamma_\alpha} \boldsymbol{v}\cdot\boldsymbol{n}^{[\alpha]}\,\mathrm{dS}_y\,, \quad \forall \boldsymbol{v} \in \mathbf{H}^1_\#(Y) \\ \langle q,\, \mathrm{div}_y \boldsymbol{\omega}^\alpha\rangle_{Y_3} + \Delta t\, c_{Y_3}\left(\pi^\alpha,\, q\right) = 0\,, \quad \forall q \in H^1_{\#0}(Y_3)\,, \\ \pi^\alpha = \delta_{\alpha\beta} \quad \text{a.e. on } \Gamma_\beta\,. \end{aligned} \tag{11}$$

3. Particular responses for given $\tilde{\boldsymbol{\tau}}$ and $\tilde{p}_3$: find $(\boldsymbol{u}^P, p^P) \in \mathbf{H}^1_\#(Y) \times H^1_{\#0}(Y_3)$ such that

$$\begin{aligned} a_Y\left(\boldsymbol{u}^P,\, \boldsymbol{v}\right) - \left\langle p^P,\, \mathrm{div}_y \boldsymbol{v}\right\rangle_{Y_3} = -\int_Y \tilde{\boldsymbol{\tau}} : e_y(\boldsymbol{v}) J^{-1}\mathrm{d}y\,, \quad \forall \boldsymbol{v} \in \mathbf{H}^1_\#(Y) \\ \left\langle q,\, \mathrm{div}_y \boldsymbol{u}^P\right\rangle_{Y_3} + \Delta t\, c_{Y_3}\left(p^P,\, q\right) = -\Delta t c_{Y_3}\left(\tilde{p}_3,\, q\right)\,, \quad \forall q \in H^1_{\#0}(Y_3)\,. \end{aligned} \tag{12}$$

4. In the channels $\alpha = 1, 2$ the corrector basis functions η^k_α, $k = 1, 2, 3$ satisfy:

$$c_{Y_\alpha}\left(\eta^k_\alpha + y_k,\, q\right) = 0\,, \quad \forall q \in H^1_\#(Y_\alpha)\,. \tag{13}$$

3.3 Macroscopic equations of the time increment

The microscopic responses introduced in (10)-(13) are employed to compute the homogenized coefficients $A_{ijkl}, B_{ij}, G^\beta_\alpha, C^\beta_{ij}, Q_{ij}$ and the stress S_{ij} which are now listed; they constitute the homogenized (macroscopic) equations:

- Effective visco-elastic modulus (involving time step Δt)

$$A_{ijkl} = \frac{1}{|Y|} a_Y\left(\boldsymbol{\omega}^{kl} + \boldsymbol{\Pi}^{kl},\, \boldsymbol{\omega}^{ij} + \boldsymbol{\Pi}^{ij}\right) + \Delta \frac{1}{|Y|} t c_{Y_3}\left(\pi^{kl},\, \pi^{ij}\right)\,. \tag{14}$$

- Effective Biot poroelasticity tensor

$$B^\alpha_{ij} = \frac{|Y_\alpha|}{|Y|}\delta_{ij} + \frac{1}{|Y|}\left\langle \pi^\alpha,\, \mathrm{div}_y \boldsymbol{\Pi}^{ij}\right\rangle_{Y_3} - \frac{1}{|Y|} a_Y\left(\boldsymbol{\omega}^\alpha,\, \boldsymbol{\Pi}^{ij}\right)\,, \tag{15}$$

- Averaged total Kirchhoff stress (in the updated reference configuration)

$$S_{ij} = \frac{1}{|Y|}\int_Y \boldsymbol{\tau}^{\rm tot} J^{-1}{\rm d}y \ . \tag{16}$$

- Effective retardation stress

$$Q_{ij} = \frac{1}{|Y|}\left[a_Y\left(\boldsymbol{u}^P,\, \boldsymbol{\Pi}^{ij}\right) - \left\langle p^P,\, {\rm div}_y \boldsymbol{\Pi}^{ij}\right\rangle_{Y_3}\right] \ , \tag{17}$$

- Effective channel permeability (of the sector β):

$$C^\beta_{ij} = \frac{1}{|Y|} c_{Y_\beta}\left(\pi^l + y_l,\, \pi^k + y_k\right) \ , \tag{18}$$

  where π^l solves the autonomous local problem (13).

- Perfusion coefficient – inter-sector permeability

$$G^\alpha_\beta = \frac{1}{|Y|}\int_{\Gamma_\alpha}\left(\boldsymbol{K}^3\cdot\nabla_y\pi^\beta\right)\cdot\boldsymbol{n}^{[3]}\,{\rm dS}_y + \frac{1}{\Delta t}\frac{1}{|Y|}\int_{\Gamma_\alpha}\boldsymbol{\omega}^\beta\cdot\boldsymbol{n}^{[\alpha]}\,{\rm dS}_y \ , \tag{19}$$

- Effective discharge due to deformation of the reference state (in the updated configuration)

$$g^{\rm eff}_\alpha = \frac{1}{|Y|}\int_{\Gamma_\alpha}\left(\boldsymbol{K}^3\cdot\nabla_y(p^P+\tilde{p}^3\right)\cdot\boldsymbol{n}^{[3]}\,{\rm dS}_y + \frac{1}{\Delta t}\frac{1}{|Y|}\int_{\Gamma_\alpha}\boldsymbol{u}^P\cdot\boldsymbol{n}^{[\alpha]}\,{\rm dS}_y \ , \tag{20}$$

The macroscopic incremental problem is solved for displacements $\Delta\boldsymbol{u}^0 \in \boldsymbol{V}(\Omega)$ and pressures $\Delta p^0_\beta \in H^1(\Omega)$, $\beta = 1, 2$ which satisfy the following equations:

Equilibrium equation:

$$\int_\Omega\left(A_{ijkl}\partial_l\Delta u^0_k - \sum_{\alpha=1,2}B^\alpha_{ij}\Delta p^0_\alpha\right)\partial_j v^0_i{\rm d}x = L(\boldsymbol{v}^0) - \int_\Omega\left(Q_{ij}+S_{ij}\right)\partial_j v^0_i{\rm d}x \tag{21}$$

for all $\boldsymbol{v}^0 \in \boldsymbol{V}_0(\Omega)$,

Diffusion equations: for $\beta = 1, 2$,

$$\int_\Omega q^0_\beta\left(B^\beta_{ij}\partial_j\Delta u^0_i + \sum_{\alpha=1,2}G^\beta_\alpha\Delta p^0_\alpha\right){\rm d}x + \int_\Omega C^\beta_{kl}\partial_l(\Delta p^0_\beta + p^0_\beta)\,\partial_k q^0_\beta{\rm d}x = -\int_\Omega g^{\rm eff}_\beta q^0_\beta{\rm d}x \ , \tag{22}$$

for all $q^0_\beta \in H^1(\Omega)$. The homogenized problem involves two diffusion equations describing perfusions in the two compartments labeled by $\beta = 1, 2$. This is the direct consequence of a) the dual porosity in Y_3 and b) topology of the decomposition of Y with Y_1 disconnected from Y_2.

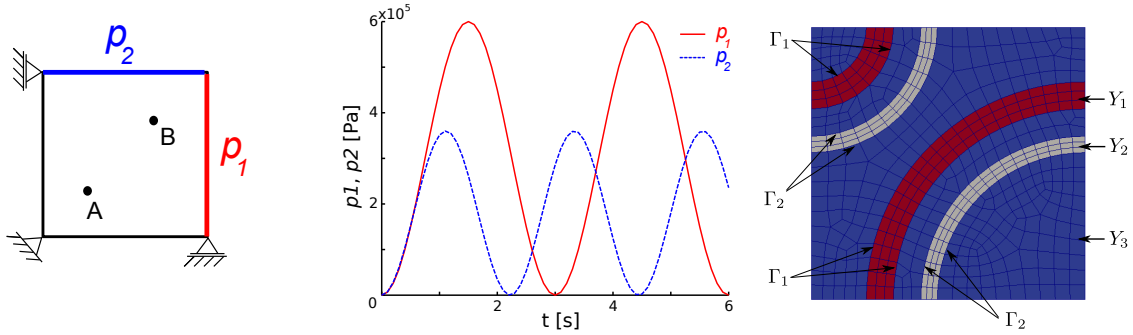

Figure 1: A macroscopic tissue 2D-sample with two labeled points (left), prescribed perfusion pressures $p_1(t)$, $p_2(t)$ as constant along two different faces (center) and the 2D microstructure (right).

3.4 Updating the local microstructures

We shall now explain the time stepping algorithm which is used to compute deformation of the medium and fluid redistribution in the pores at discrete time levels. At a certain time level (labeled by $^{(t)}$), the macroscopic configuration is represented by the triplet $\mathcal{M}^{(t)} \equiv \{\Omega^{(t)}, F_{ij}^{(t)}(x), p_\alpha^{(t)}(x) |\ x \in \Omega^{(t)}\}$ and the microscopic configurations are given by $\mathcal{C}^{(t)}(x)$, are given, see (3). The coupled micro-macro algorithm involves the following steps:

1. Given $\mathcal{M}^{(t)}$ and $\mathcal{C}^{(t)}(x)$ for $x \in \Omega^{(t)}$, solve the microscopic problems (10)-(13), then compute all the homogenized coefficients: $A_{ijkl}, B_{ij}, G_\alpha^\beta, C_{ij}^\beta, Q_{ij}$ and stress S_{ij}.
2. Compute Δu^0 and Δp_α^0 by solving (21)-(22).
3. Update macroscopic configuration $\mathcal{M}^{(t)} \to \mathcal{M}^{(t+\Delta t)}$, $\Omega^{(t+\Delta t)} := \Omega^{(t)} + \{\Delta u^0\}$.
4. For a.a. points $x \in \Omega^{(t)}$ update $\mathcal{C}^{(t)}(x) \to \mathcal{C}^{(t+\Delta t)}(\boldsymbol{x} + \Delta \boldsymbol{u}^0(x))$; this step consists in:

(a) Updating deformation and deformed domain

$$\begin{aligned} \Delta u_i^* &:= (\delta_{ir}\delta_{js} y_j + \omega_i^{rs})\ \partial_s^x \Delta u_r^0(x) + \sum_{\alpha=1,2} \omega_i^\alpha \Delta p_\alpha^0(x) + u_i^P\ , \\ f_{ij} &:= \delta_{ij} + \partial_j^y \Delta u_i^*\ , \\ F_{ij} &:= f_{ik} F_{kj}\ , \\ Y^{(t+\Delta t)}(x) &:= Y^{(t)}(x) + \{\Delta \boldsymbol{u}^*\}\ , \end{aligned} \tag{23}$$

where F_{ij} is the total deformation gradient at the microscopic level.

(b) Updating pressure fields for $x \in \Omega^{(t)}$:

- update the channel pressures:

$$\begin{aligned} \Delta \tilde{p}_\alpha &= \Delta p_\alpha^0 + \varepsilon_0 \eta_\alpha^k \partial_k^x \Delta p_\alpha^0\ , \\ \tilde{p}_\alpha^{(t+\Delta t)} &= \tilde{p}_\alpha^{(t)} + \Delta \tilde{p}_\alpha\ , \end{aligned} \tag{24}$$

where $\varepsilon_0 > 0$ is a given scale of the microstructure.

- update the dual porosity pressure:

$$\Delta\tilde{p}_3 = \pi^{rs}\partial_s^x \Delta u_r^0(x) + \sum_{\alpha=1,2} \pi^\alpha \Delta p_\alpha^0(x) + p^P \,, \qquad \tilde{p}_3^{(t+\Delta t)} = \tilde{p}_3^{(t)} + \Delta\tilde{p}_3 \,. \tag{25}$$

Now $\mathcal{C}^{(t+\Delta t)}(\boldsymbol{x} + \Delta\boldsymbol{u}^0(x))$ for $x \in \Omega^{(t)}$ is constituted by $(23)_{3,4}$ and $(25)_2$.

5. Stop, when maximum time is reached, or return to step 1 with $t := t + \Delta t$.

Material parameters depend on local strain and stress, in general, so they are defined in the updated local microscopic configuration $\mathcal{C}^{(t)}(x)$.

domain	shear modulus μ [Pa]	permeability coef. c_{perm} [m^2/(Pa·s)]
matrix Y_3	1×10^6	1×10^{-9}
channel Y_1	6×10^5	1×10^{-8}
channel Y_2	4×10^5	2×10^{-8}

Table 1: Material parameters at the microscale; the permeability is isotropic, $K_{ij}^k = c_{perm}^k \delta_{ij}$, in all subdomains Y_k, $k = 1, 2, 3$. Thus, for scale $\varepsilon_0 = 0.01$, the matrix permeability is $c_{perm}^{\varepsilon_0,3} = \varepsilon_0^2 c_{perm}^3 = 10^{-13}$.

4 EXAMPLE – PERFUSION IN 2D

The two-scale model of the perfusion is now implemented in the in-house developed FE code **SfePy** , [1] which was developed using some techniques already tested on problems of large deforming solids, as reported in papers [5, 3]. Here we report a simple simulation in 2D, see Tab. 1 for the material parameters used at the microscopic scale. The specimen is loaded just by two perfusion pressures varying in time and supported at three nodes as illustrated in Fig. 1. The microstructure is (initially) periodic with the reference cell Y containing two systems of curved channels. The material parameters defining the microscopic problems are listed in Tab. 1; note that the "real permeability" in the dual porosity Y_3 is 10^{-4} times smaller, being the ε_0^2-multiple, where $\varepsilon_0 = 0.01$ in our situation. (We used nonphysiological values for testing the model on "non-realistic" 2D examples; in this case the elasticity in the channels must be taken larger.)

The simulation was performed with the time increment $\Delta t = 0.2\,\mathrm{s}$, which is sufficiently large to use the Q1-Q1 finite element discretization for both the displacements and the pressures (note that too small step Δt induces "numerical incompressibility" and another mixed element would have to be used, like Q2-Q1). The microstructures are updated for each Gauss point of the macroscopic domain (discretized using 16 elements, i.e. $16\times4 = 64$ microstructures updated at each time level, in our example), 30 time levels were evaluated. The approximate wall-time of the simulation on one single-processor PC was ≈30 minutes.

Some numerical illustrations are displayed in Figs. 2-4. The tissue perfusion at a macroscopic position $x \in \Omega$ can be deduced form the pressure difference, see Fig. 3.

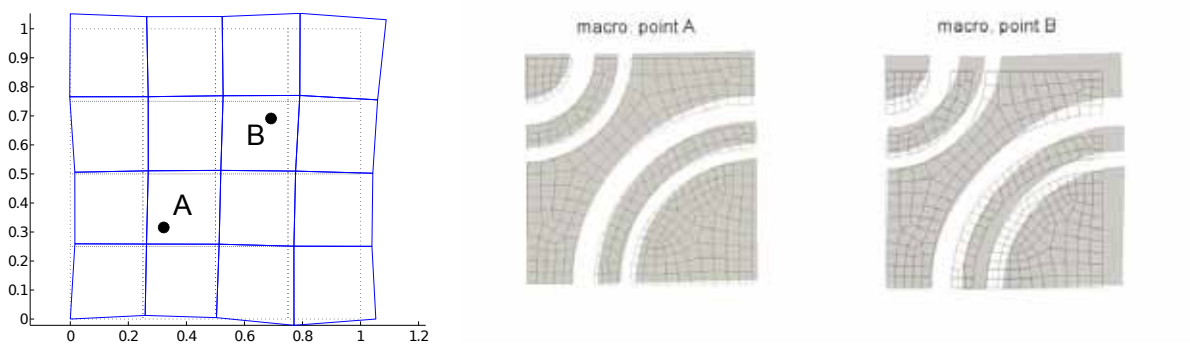

Figure 2: Deformation of the macroscopic specimen (left) and the local deformed configurations $Y(x^A)$ and $Y(x^B)$ for the labeled positions. We recall the fixed corner points of the specimen, see Fig. 1.

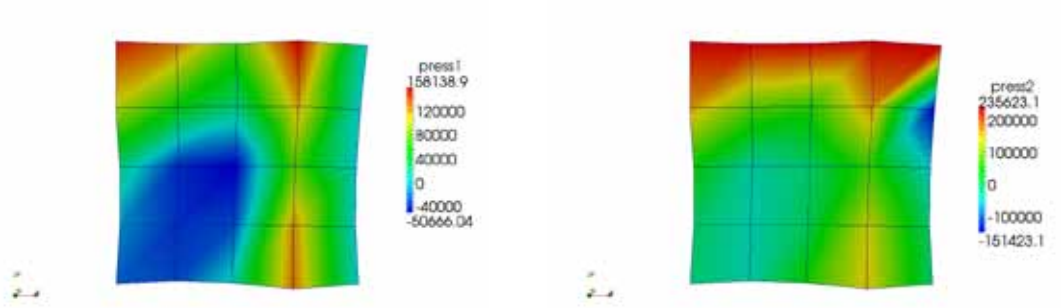

Figure 3: Macroscopic distribution of two perfusion pressures p_1 and p_2 in the deformed domain Ω (evaluated at the final time of the simulation).

5 CONCLUSIONS

We combined the double-porous media approach employed in homogenization of the linear models [6, 7] with the large deformation description defined using the updated Lagrangian formulation [5]. The fluid redistribution at the macroscopic scale between the two channel systems is proportional to the difference of these pressures. At the microscopic scale the fluid flows can be recovered using the corrector functions.

The fluid-solid interactions governed by the poroelasticity model of Biot are responsible for viscoelastic effects observed at the macroscopic scale, which are represented in the global macroscopic homogenized model by the retardation stress Q_{ij}. It is worth noting that apart of the homogenized permeabilities C_{ij}^{β}, all the other homogenized coefficients of the incremental problem depend on the time step Δt by virtue of the microscopic problems (10)-(12). In the linear case, the homogenized model involves the homogenized kernels of the time-convolution integrals, inducing the fading memory effects [6, 7].

Some effective strategy is required to tackle the number of the microscopic problems that have to be solved at each time step to recover the effective (homogenized) material constants. In [3] we have presented a parallel micro-macro algorithm, attempting to

address this issue.

The numerical simulations will be extended for 3D problems and some more realistic data will be used to validate the homogenized model. Since experimental results are unavailable, the model and the two-scale computational approach will be verified using a "non-homogenized" model (the reference model) based on a direct FE discretization of the system (1)-(2), whereby the geometry will be extremely complex (even for some higher scale parameters ε_0). To obtain a numerical solution for the reference model, some domain-decomposition techniques will be employed, including parallel algorithms.

Acknowledgment This research is supported by research projects GACR 106/09/0740 and MSM 4977751303 of the Czech Republic.

REFERENCES

[1] Cimrman, R. etal, "Software, finite element code and applications", SfePy home page, http://sfepy.kme.zcu.cz,http://sfepy.org, (2009).

[2] Cioranescu, D. and Donato, P. *An Introduction to Homogenization*, Oxford Lecture Series in Mathematics and its Applications 17, Oxford University Press, Oxford, (1999).

[3] Rohan, E., Cimrman, R. and Lukeš, V. Numerical modelling and homogenized constitutive law of large deforming fluid saturated heterogeneous solids. *Computers and Structures* 84 (2006), 1095-1114.

[4] Rohan, E. and Lukeš, V. Homogenization of perfusion in large-deforming medium using the Updated Lagrangean Formulation. *In Proc. 7th Int. Conf. ECT 2010*, Saxe-Coburg Publ., Edinburgh, Paper 83 (2010).

[5] Rohan, E. Modelling large deformation induced microflow in soft biological tissues. *Theor. and Comp. Fluid Dynamics* 20 (2006), 251–276.

[6] Rohan, E. and Cimrman, R. Multiscale FE simulation of diffusion-deformation processes in homogenized dual-porous media. *Math. and Comp. Simul.*, In Press (2011)

[7] Rohan, E. and Cimrman, R. Two-scale modelling of tissue perfusion problem using homogenization of dual prous media. *Int. Jour. Multiscale Comput. Eng.*, 8 (2010), 81-102.

[8] Takano, N., Ohnishi, Y., Zako, M. and Nishiyabu, N. The formulation of homogenization method applied to large deformation problem for composite materials, *International Journal of Solids and Structures* 37, (2000), 6517-6535.

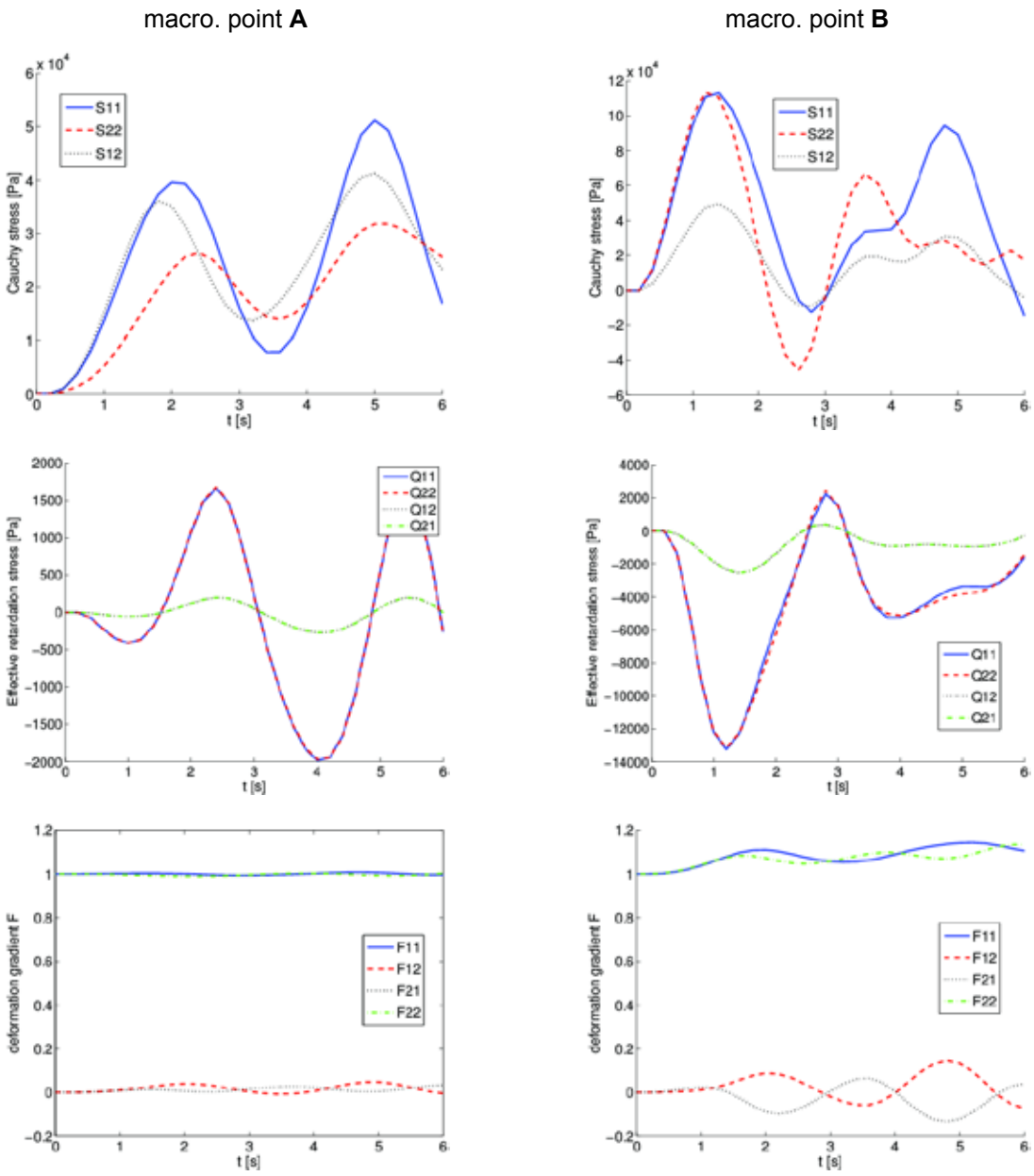

Figure 4: Macroscopic quantities S_{ij}, Q_{ij} and F_{ij} evaluated in time at points A (left column) and B (right column) of the macroscopic specimen.